

Dissociation Between the Epileptogenic Lesion and Primary Seizure Onset Zone in the Tetanus Toxin Model of Temporal Lobe Epilepsy

Jan CHVOJKA^{1,2}, Jan KUDLACEK¹, Karolina LISKA¹, Aakash PANT¹,
John G.R. JEFFERYS¹, Premysl JIRUSKA¹

¹Department of Physiology, Second Faculty of Medicine, Charles University, Prague, Czech Republic, ²Department of Circuit Theory, Faculty of Electrical Engineering, Czech Technical University in Prague, Prague, Czech Republic

Received November 12, 2023

Accepted February 13, 2024

Summary

Despite extensive temporal lobe epilepsy (TLE) research, understanding the specific limbic structures' roles in seizures remains limited. This weakness can be attributed to the complex nature of TLE and the existence of various TLE subsyndromes, including non-lesional TLE. Conventional TLE models like kainate and pilocarpine hinder precise assessment of the role of individual limbic structures in TLE ictogenesis due to widespread limbic damage induced by the initial status epilepticus. In this study, we used a non-lesional TLE model characterized by the absence of initial status and cell damage to determine the spatiotemporal profile of seizure initiation and limbic structure recruitment in TLE. Epilepsy was induced by injecting a minute dose of tetanus toxin into the right dorsal hippocampus in seven animals. Following injection, animals were implanted with bipolar recording electrodes in the amygdala, dorsal hippocampus, ventral hippocampus, piriform, perirhinal, and entorhinal cortices of both hemispheres. The animals were video-EEG monitored for four weeks. In total, 140 seizures (20 seizures per animal) were analyzed. The average duration of each seizure was 53.2 ± 3.9 s. Seizure could initiate in any limbic structure. Most seizures initiated in the ipsilateral (41 %) and contralateral (18 %) ventral hippocampi. These two structures displayed a significantly higher probability of seizure initiation than by chance. The involvement of limbic structures in seizure initiation varied between individual animals. Surprisingly, only 7 % of seizures initiated in the injected dorsal hippocampus. The limbic structure recruitment into the seizure activity wasn't random and displayed consistent patterns of early recruitment of hippocampi and entorhinal cortices. Although ventral hippocampus represented the

primary seizure onset zone, the study demonstrated the involvement of multiple limbic structures in seizure initiation in a non-lesional TLE model. The study also revealed the dichotomy between the primary epileptogenic lesion and main seizure onset zones and points to the central role of ventral hippocampi in temporal lobe ictogenesis.

Key words

Temporal lobe epilepsy • Hippocampus • Entorhinal cortex • Seizure onset • Neural networks

Corresponding author

P. Jiruska, Department of Physiology, Second Faculty of Medicine, Charles University, Plzenska 311, Prague 5, CZ-15006, Czech Republic. E-mail: jiruskapremysl@gmail.com or premysl.jiruska@lfmotol.cuni.cz

Introduction

Epilepsy represents a cerebral network disorder where seizures emerge from complex interactions between the components of the epileptic network rather than from one specific brain region [1,2]. In temporal lobe epilepsy (TLE), the limbic structures and their connections with other brain areas represent the crucial components of the abnormal epileptic networks. The large interconnectivity of limbic structures plays a crucial role in physiological functions, and limbic connectivity alterations represent a structural substrate contributing to high epileptogenicity and ictogenicity of the limbic system [3]. In TLE, the multiple limbic structures of both

hemispheres become involved in the genesis of interictal and ictal activity. TLE is classified into various subsyndromes in humans according to the level of involvement of individual limbic structures that also determine the outcome of epilepsy surgery [4,5]. The hippocampus is the most prominent limbic structure involved in TLE, and hippocampal sclerosis is one of the most common epileptogenic lesions and the most common source of seizures in TLE [6]. Seizure onsets can occur in entorhinal cortex, amygdala, or piriform cortex but less frequently than in the hippocampus [5]. The degree of involvement of individual limbic structures varies between patients but also within individuals. Human and animal studies demonstrate that multiple limbic structures can be involved in seizure genesis in the same patient or animals, and seizure onset can change in the long term [1,7-9]. The high seizure onset variability explains why epilepsy surgery fails to provide seizure freedom in a significant proportion of patients with temporal lobe epilepsy. Non-lesional TLE is the most challenging form of TLE from the clinical perspective [10]. The absence of epileptogenic lesions in MRI (hippocampal or mesiotemporal lobe sclerosis, low-grade tumor) prevents the non-invasive identification of the plausible seizure onset zone. Therefore, patients with non-lesional TLE often undergo invasive exploration with intracranial electrodes to map the epileptic network and identify the most epileptogenic structures [11]. Despite advances in presurgical diagnostics, the success rate of post-surgical freedom remains less than optimal [10]. Experimental knowledge on the organization of TLE networks and the pathophysiology of TLE was obtained mainly from the status epilepticus models induced by pilocarpine or kainic acid models [12-17]. It is well documented that prolonged status epilepticus causes severe structural damage (cell loss, axonal sprouting, gliosis) affecting multiple limbic structures [13-16]. Multisite damage represents one of the disparities between human TLE and animal models and hinders the precise evaluation of individual limbic structure contributions to the TLE network [18].

The experimental model of non-lesional TLE induced by intrahippocampal injection of a minute dose of tetanus toxin (TeNT) is characterized by the absence of initial status epilepticus and the absence of severe cell loss or hippocampal sclerosis [19,20]. In this study, we took advantage of the unique nature of the TeNT model to explore the network organization and role of limbic structures in TLE ictogenesis. The results demonstrate

that seizure can initiate in multiple limbic structures despite a localized epileptogenic lesion in the dorsal hippocampus. Surprisingly, the most common seizure onset zones were the ipsilateral and contralateral ventral hippocampi, while the injected dorsal hippocampus played a minimal role in seizure initiation. Similarly to humans, the seizure onset varied between animals with various degrees of involvement of individual limbic structures in seizure genesis. The observed dichotomy between the primary lesion and principal seizure onset zone could be attributed to the ventral hippocampus's high endogenous epileptogenic potential and interconnectivity that may predispose the ventral hippocampus to generate seizures in response to distant lesions [21-24].

Materials and Methods

TLE induction and electrode implantation

Seven adult male Wistar rats 250-400 g underwent implantation of multiple electrodes across the limbic structures, followed by long-term video-EEG monitoring. All experiments were performed under the Animal Care and Animal Protection Law of the Czech Republic, fully compatible with the European Union directive 2010/63/EU guidelines. The protocol was approved by the Ethics Committees of the Second Faculty of Medicine (Project License No. MSMT-31765/2019-4). Animals were housed in groups under standard and enriched conditions in a room with a controlled temperature ($22\pm 1^\circ\text{C}$) and a 12/12 h light/dark cycle in open cages, enabling all but physical interaction.

Animals were anesthetized using 5 % isoflurane in a plexiglass chamber. Then, the rat was fixed in the stereotaxic apparatus, and the anesthesia was maintained by 2.5 % isoflurane, slowly decreasing to 1.5 %. TLE was induced by injection of 10 ng of tetanus toxin (Quadragech Diagnostic Ltd, Epsom, UK, No #190A) to the right CA3 region of dorsal hippocampus at the coordinates AP -4.1 mm, L 3.9 mm from bregma and D 4.2 mm from the skull surface. Recording electrodes were implanted in the key structures of the limbic system using stereotaxic atlas [25], according to Table 1. Four animals had implanted additional electrodes in the dorsal hippocampal CA3 and subiculum, which were, however, not analyzed in this study (marked by gray shading in the table).

Table 1. Stereotactic coordinates of the implanted limbic structures. Units are millimeters. Positive values are rostral from bregma, while negative values are caudal from bregma. AP – antero-posterior.

Brain structure	AP	Lateral	Depth
<i>Piriform cortex</i>	0.2	4.2	8.2
<i>Amygdala</i>	-2.8	4.8	8.6
<i>Perirhinal cortex</i>	-2.8	6.2	7.4
<i>Dorsal dentate gyrus</i>	-4.6	2.6	3.3
<i>Ventral hippocampus</i>	-5.5	4.8	7.1
<i>Entorhinal cortex</i>	-8.0	5.0	7.0
<i>Dorsal CA3</i>	-4.1	4.2	4.4
<i>Dorsal subiculum</i>	-6.0	2.0	3.2

EEG recording and analysis

Following a 5-day recovery period, the animals were subjected to video-EEG monitoring for at least three weeks. Two different recording setups were used. The Neuralynx setup consisted of a headstage unity-gain amplifier HS-27 (Neuralynx, Bozeman, Montana, USA) and a Lynx-8 amplifier (Neuralynx, Bozeman, Montana, USA) set to a gain of 196, high-pass filter at 0.1 Hz and a low-pass filter at 3 kHz. The signal was then digitized using a Power 1401 analogue-digital converter (Cambridge Electronic Design, Cambridge, UK) at the sampling frequency of 10 kHz and 16-bit resolution and recorded to a computer using Spike2 software (Cambridge Electronic Design, Cambridge, UK). The synchronized video was recorded by Spike2 using a USB webcam. Signals recorded using the Intan setup were amplified, analog-filtered, and digitized by an RHD2132 headstage board (Intan Technologies, Los Angeles, California, USA). The digitized signals were transferred *via* swivel using the SPI bus to the RHD2000 evaluation board, which was connected to a computer *via* USB. The analog high-pass filter was set to 0.1 Hz and the low-pass filter to 1.7 kHz. The sampling frequency was 5 kHz, and the resolution was 16 bit. Custom-made software was used for EEG recording. The synchronized video was recorded using a USB camera.

Seizure onset detection and recruitment analysis

From each of the eight animals, we have chosen their first 20 seizures lasting >10 s for detailed evaluation of electrographic seizure onset times. Seizures and seizure onsets were visually identified in each electrode using custom-written Matlab scripts (Mathworks Inc., USA). Seizure onset was defined as the earliest

appearance of a persistent and profound change in EEG background activity that developed into clear ongoing seizure activity. Electrode with the earliest signal change was marked as a seizure onset (initiation) zone. The timing of seizure onset in each electrode was used to estimate the time delays of seizure propagation and limbic structure recruitment pattern. Seizure onsets time generated a 12×20 matrix (12 structures × 20 seizure onsets) from which propagation time delays and limbic structure recruitment plots were generated. We computed the “recruitment pathway” for each seizure onset as a vector of limbic structure ranking according to observed recruitment delays. Recruitment pathways were then compared to random pathways to assess significance.

Statistical analysis

Unless otherwise stated, all results and graphs are shown as mean ± s.e.m (median). All tests used level $\alpha=0.05$ to determine the statistical significance. No data points were excluded. We did not implement any statistical approach to a priori define the sample size, but it corresponds to sample sizes that are generally used in this field of research.

Measured seizure onset frequencies were first compared to uniform frequencies using a one-way chi-square test, followed by an analysis of confidence intervals.

The PERMANOVA method of 10000 iterations was used in the recruitment analysis to determine the statistical significance of dissimilarity between observed and random recruitment pathways. The dissimilarity was evaluated utilizing Kendall's Tau rank correlation as the distance metric. Recorded data and analytical tools used in this study are available from the corresponding author upon request.

Results

TeNT epileptic syndrome

All seven animals developed an epileptic syndrome characterized by recurrent spontaneous seizures (Fig. 1A). Seizures were behaviorally accompanied by staring, loss of awareness, and facial automatisms (sniffing, chewing; Racine scale 1-2) [26]. The seizure could progress further into a convulsive phase accompanied by motor phenomena ranging from forelimb clonus to rearing and ictal falling (Racine scale 3-5). A substantial number of seizures were electrographic without any apparent change in the

animal's behavior. Wet dog shakes often followed the seizure termination. During the period between seizures, interictal epileptiform discharges of various morphologies were present in recordings.

Seizure onset analysis

In total, 140 seizures from seven male rats were analyzed. The average duration of each seizure was 53.2 ± 3.9 s. The seizure onset pattern was characterized as hypersynchronous in all seizures (Fig. 1B). It manifested by initial high-amplitude discharge (heralding spike), often with superimposed high-frequency oscillations. Spatially, the initial discharge occurred simultaneously in multiple limbic structures. Low-frequency, high-amplitude periodic spikes followed the heralding discharge. Using the onset of the heralding spike, we determined the seizure onset in each recorded limbic structure. The analysis of seizure onset and time delays between each limbic structure recruitment into ictal activity allowed us to determine the major seizure onset structures and pattern of seizure propagation in this model of temporal lobe epilepsy.

The results showed that the seizure onset structure was not stable, and seizures could initiate between five to seven limbic structures in each animal, although with various proportions of initiation (Fig. 2 and 3A). On average, 55 ± 3 (55) % of seizures were initiated in the limbic structures of the right hemisphere (ipsilaterally to TeNT injection), while 45 ± 3 (45) % of seizures originated in the contralateral (left) limbic structures. The ipsilateral ventral hippocampus was the main seizure onset structure, with 41 ± 5 (40) % of seizures initiated in this structure (Fig. 3B, C). The proportion of ipsilateral ventral hippocampal seizure onsets varied from 30 % up to 60 % across the animals (Fig. 3A). Contralateral ventral hippocampus was the second most common seizure onset structure 18 ± 3 (20) % and was above chance levels (Fig. 3B). The other limbic structures did not cross the significance of the random initiation threshold (Fig. 3B). Surprisingly, only 6 ± 1 (5) % of seizures started from the injected right dorsal hippocampus. Dorsal and ventral hippocampi generated 75 ± 4 (75) % of all seizures (Fig. 3B, C).

Seizure propagation and limbic structure recruitment

Because of the statistically significant difference ($p < 0.001$, one-way chi-square test), we then focused on seizure onset propagation patterns of seizures generated only in ventral hippocampi. The ictal propagation maps of

the right ventral hippocampal seizures ($n=63$ seizures) suggested that the seizure propagation pattern is consistent in each animal (Fig. 4A-F) and across animals (Fig. 4H). We determined the average propagation delay for each limbic structure to quantify the propagation pattern. We then ranked the recruitment of each structure (Fig. 5A). Entorhinal cortices and hippocampal subregions demonstrated the earliest recruitment. The average delay from the right ventral hippocampus to the right and left entorhinal cortex was 17 ± 3 (9) ms and 31 ± 4 (19) ms, respectively. The contralateral ventral and dorsal hippocampi were recruited into the seizure activity with a time delay of 29 ± 4 (18) ms and 50 ± 6 (29) ms. Surprisingly, the amygdalar complex wasn't amongst the structures with the fast recruitment. The average time delay to the ipsilateral amygdala was 44 ± 7 (23) ms, and the time delay to the contralateral amygdala was 70 ± 10 (46) ms. The results confirmed the existence of consistent propagation pathways and a consistent sequence of limbic structures' recruitment. To statistically evaluate this observation, we compared the observed recruitment pattern with surrogate data of random recruitment (Fig. 5B-D). The analysis demonstrated statistically significant dissimilarity between propagation pathways of seizures originating from the right ventral hippocampus (PERMANOVA, pseudo-F test statistic of 2.84, p-value of 0.011) compared to random recruitment. Propagation patterns (Fig. 4I-P), average propagation delays (Fig. 6A), and limbic structure recruitment sequence (Fig. 6B-E) of left ventral hippocampal seizures ($n=28$ seizures) demonstrated that they also followed the consistent paths and recruitment sequences (PERMANOVA, pseudo-F test statistic of 2.87, p-value of 0.015) that mirrored recruitment patterns of the right ventral hippocampus. The average propagation delay to the left and right entorhinal cortex was 12 ± 2 (10) ms and 29 ± 8 (21) ms, respectively. The contralateral ventral and dorsal hippocampi were recruited into the seizure activity with a time delay of 26 ± 8 (15) ms and 34 ± 6 (27) ms (Fig. 6A).

Discussion

One of the reasons behind the unsatisfactory results of TLE surgery is that the temporal lobe epileptic network can be spatially extensive, and critical components of the network can differ in each subsyndrome [1,5,27-30]. TLE networks involve multiple structures of the limbic system, ranging from the hippocampus to entorhinal and perirhinal cortices

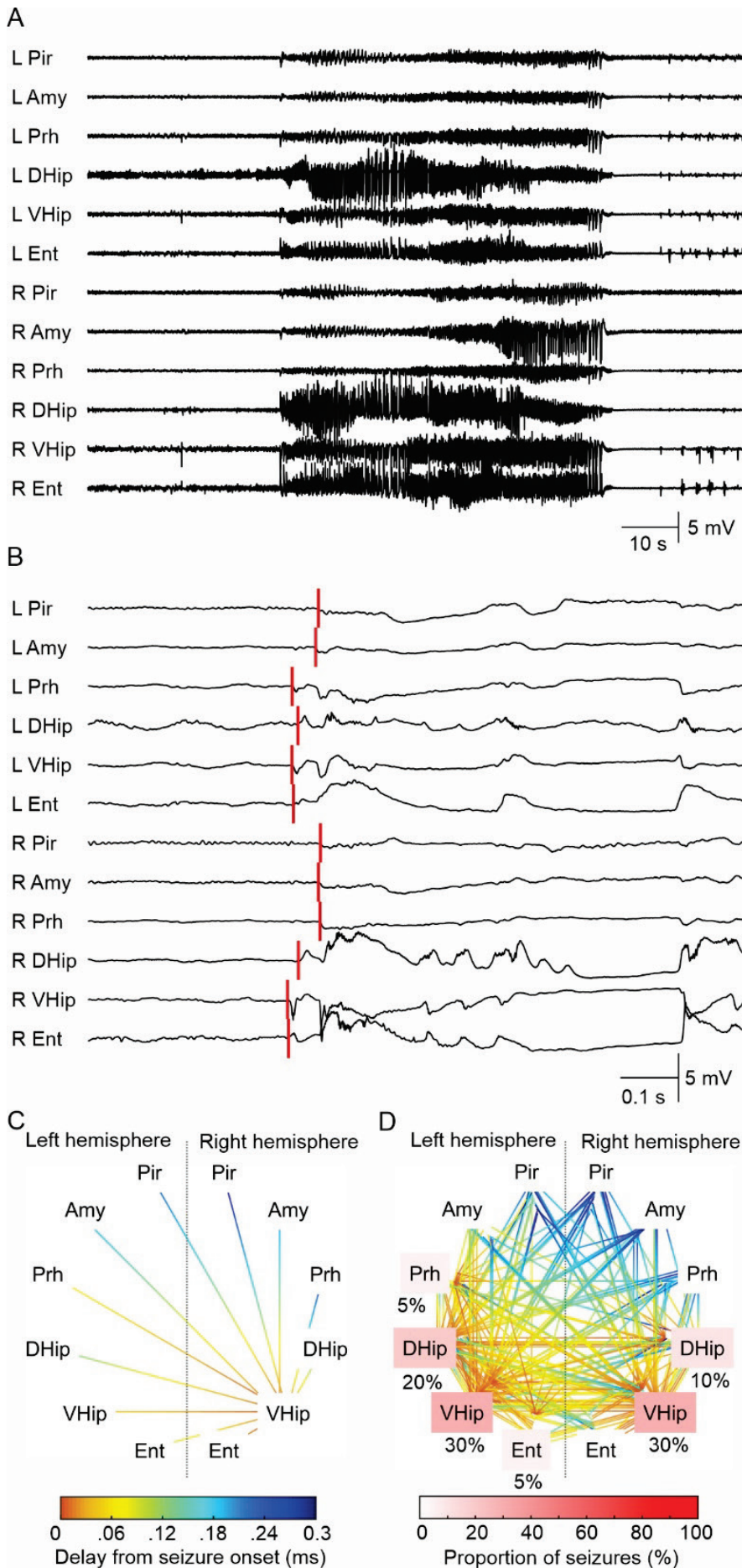


Fig. 1. Seizure and seizure onset analysis. **(A)** An example of a seizure in the tetanus toxin model induced by the dorsal hippocampal TeNT injection. Seizure activity rapidly propagates across the limbic structures of both hemispheres. The seizure initiation displays features of hypersynchronous onset characterized by the initial high-amplitude discharge (heralding spike), often with superimposed high-frequency activity. Seizure terminates synchronously over the wide areas of both hemispheres. **(B)** The detail of seizure onset. The initial high-amplitude (hypersynchronous) discharge rapidly spread into the limbic structures of both hemispheres. The red lines mark visually determined seizure onset in each electrode. This seizure was initiated in the ipsilateral (right) ventral hippocampus. **(C)** Seizure onset and early ictal propagation analysis. The lines connect the limbic structures where the seizure activity propagates from the seizure onset structure (ventral hippocampus). The color coding reflects the propagation time. In this case, the propagation to the ipsilateral entorhinal cortex and contralateral ventral hippocampus is reflected by the hot color of the line endings. On the contrary, the propagation of ictal activity to piriform cortices of both hemispheres is slow, resulting in their late recruitment into the seizure. The cold color of the line endings reflects long propagation time and late recruitment. **(D)** The overlay of all seizure onsets ($n=20$) from one animal. In this animal, 30 % of seizures were initiated in the right ventral hippocampus, 30 % in the left ventral hippocampus, 20 % in the left dorsal hippocampus, 5 % in the left entorhinal cortex, 10 % in the right (injected) dorsal hippocampus, and 5 % from the left perirhinal cortex. The white-red color coding of the limbic structure label identifies the proportion of seizures initiated from the specific limbic structure. L – left hemisphere, R – right hemisphere, Pir – piriform cortex, Amy – amygdala, Prh – perirhinal cortex, DHip – dorsal hippocampus, VHip – ventral hippocampus, Ent – entorhinal cortex. The graph also displays the most common patterns and time delay of seizure propagation (parula color coding).

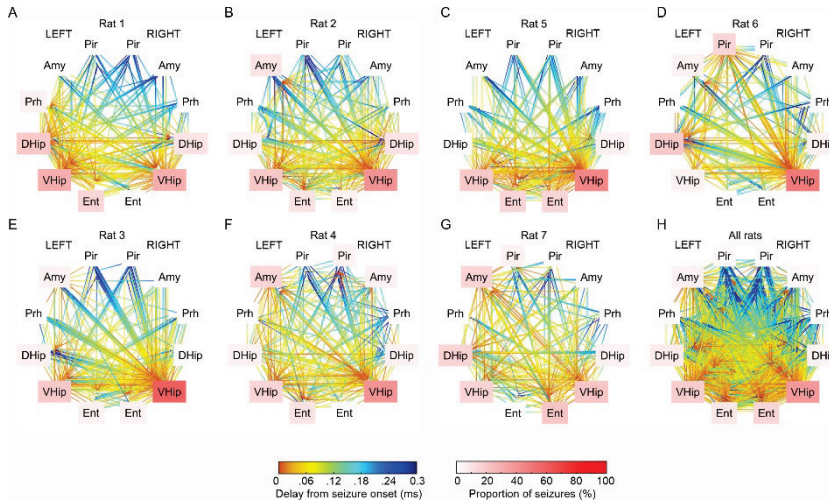


Fig. 2. Seizure onset analysis in each animal. (A-G) The proportion of limbic structures involved in seizure initiation and propagation varies across the animals. Ventral and dorsal hippocampi and entorhinal cortices of both hemispheres were the most common structures triggering seizures. (H) Overlay and propagation of all 140 seizures from all animals. L – left hemisphere, R – right hemisphere, Pir – piriform cortex, Amy – amygdala, Prh – perirhinal cortex, DHip – dorsal hippocampus, VHip – ventral hippocampus, Ent – entorhinal cortex.

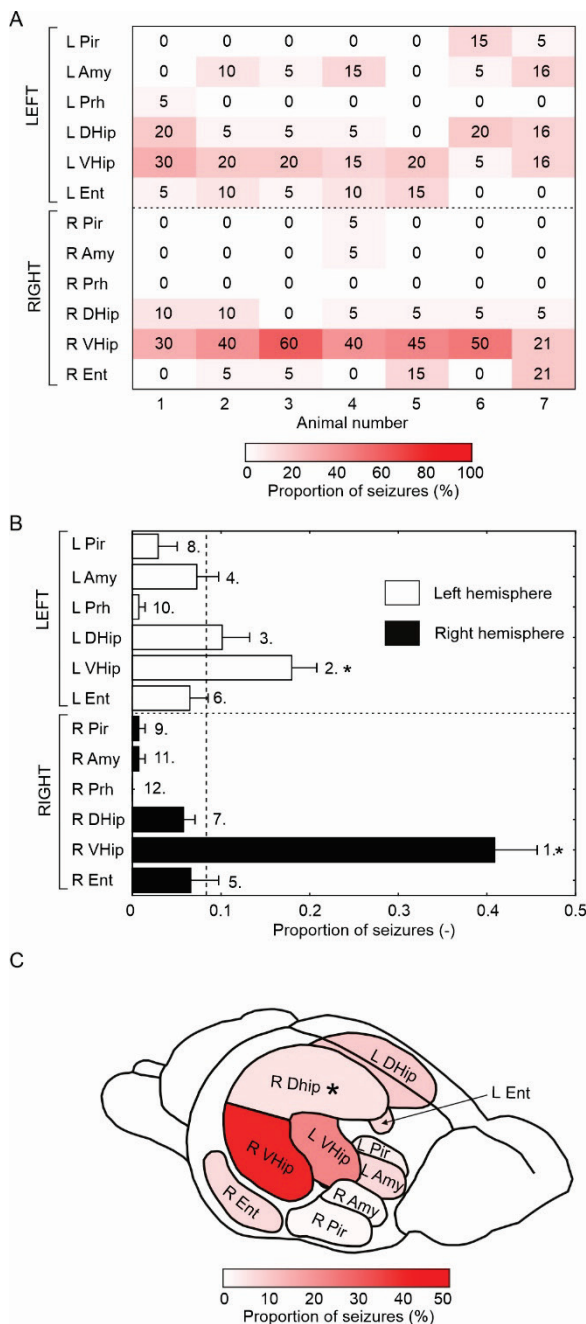


Fig. 3. Limbic structures involved in seizure initiation. (A) The matrix displays a fraction/proportion of seizures initiated in a specific limbic structure in each animal (individual column). The number and proportion of limbic structures triggering seizures varies across animals. All animals had multiple seizure onset sites, but the ipsilateral ventral hippocampus represented the main seizure onset zone in most animals. (B) The mean proportion of seizure-initiating structures. The number designates the rank, while the star marks structures where the seizure initiation is significantly ($p < 0.001$, one-way chi-square test) above the uniform distribution (vertical dashed line). Seizures initiated mainly in the ipsilateral ventral hippocampus, followed by the contralateral ventral hippocampus. (C) Schematics of a rat brain with the proportion of the individual structure involvement in seizure initiation (perirhinal cortex not shown). Asterisk marks the tetanus toxin injection to the right dorsal hippocampus. L – left hemisphere, R – right hemisphere, Pir – piriform cortex, Amy – amygdala, Prh – perirhinal cortex, DHip – dorsal hippocampus, VHip – ventral hippocampus, Ent – entorhinal cortex.

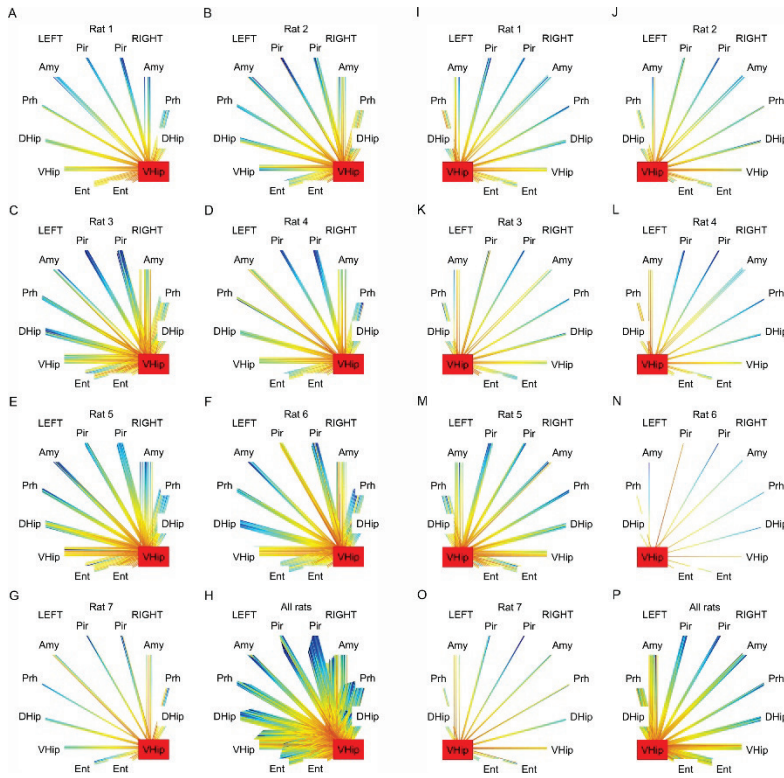


Fig. 4. Analysis of seizure pathway propagation for seizures originating from the right ventral hippocampus. (A-G) Pathways and time delays of seizure propagation for seizures initiating in the right ventral hippocampus in each animal. (H) Overlay of the seizure propagation patterns for all seizures initiated in the ipsilateral (right) ventral hippocampus (n=63). Maps show the consistent seizure recruitment/propagation pattern in each animal and across animals. (I-O) Recruitment pattern for seizures initiating in the left ventral hippocampus in each animal and across the animals (P). L – left hemisphere, R – right hemisphere, Pir – piriform cortex, Amy – amygdala, Prh – perirhinal cortex, DHip – dorsal hippocampus, VHip – ventral hippocampus, Ent – entorhinal cortex.

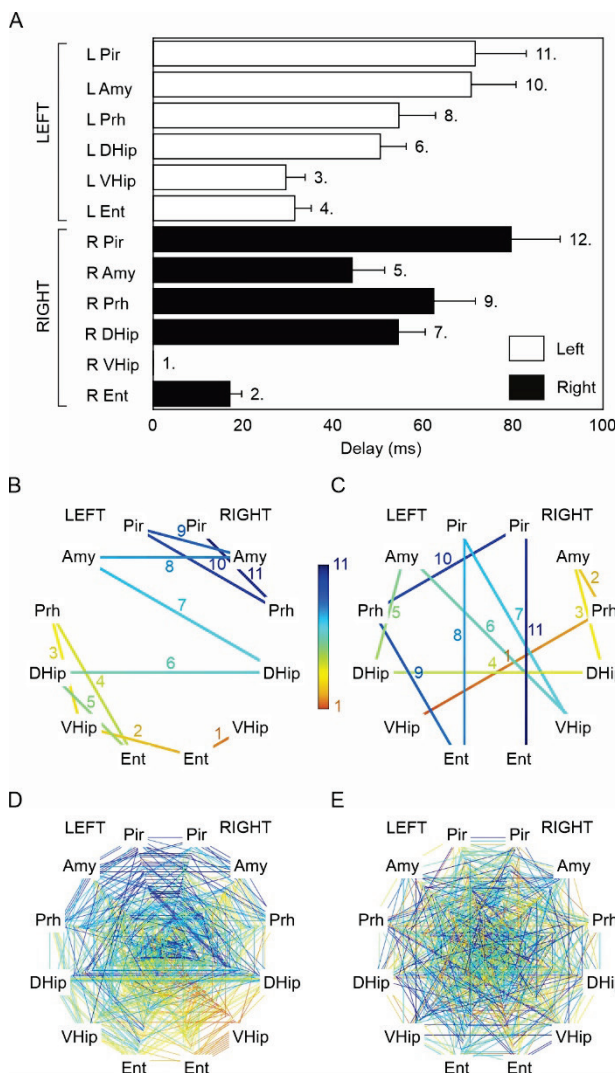


Fig. 5. Seizure pathway propagation and structure recruitment for seizures initiating in the right ventral hippocampus. (A) Average time delays show the recruitment sequence for seizures initiating in the right ventral hippocampus. The numbers mark the rank of the recruited structure. (B) Map of structure recruitment for one seizure starting in the right ventral hippocampus. The numbers and color coding mark the rank of the recruited structure. (C) Map of random recruitment. (D) Recruitment maps of all 63 seizures initiating in the right ventral hippocampus demonstrate the presence of a recruitment pattern. (E) An equal number of randomly generated recruitment maps without any recruitment pattern. L – left hemisphere, R – right hemisphere, Pir – piriform cortex, Amy – amygdala, Prh – perirhinal cortex, DHip – dorsal hippocampus, VHip – ventral hippocampus, Ent – entorhinal cortex.

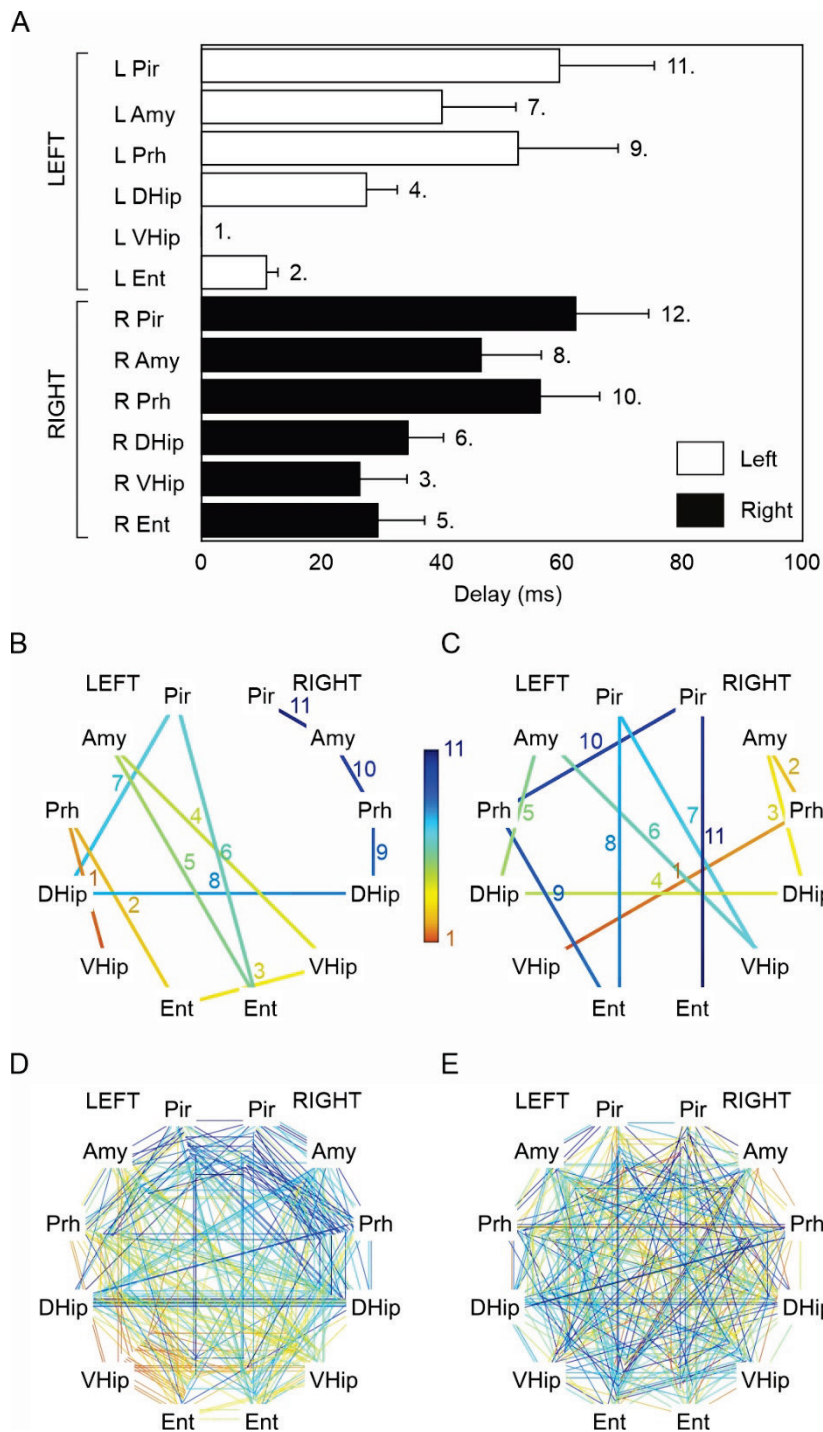


Fig. 6. Seizure pathway propagation and structure recruitment for seizures initiating in the left ventral hippocampus. (A) Average time delays show the recruitment sequence for seizures beginning in the contralateral ventral hippocampus. The numbers denote the rank of the recruited structure. (B) Map of limbic structure recruitment for a seizure originating in the left ventral hippocampus. The numbers and color coding mark the rank of the recruited structure. (C) Map of a random recruitment. (D) Recruitment maps of all 28 seizures initiating in the left ventral hippocampus demonstrate the existence of a recruitment pattern. (E) Maps of all 28 randomly generated limbic structures recruitment display the absence of any recruitment pattern. L – left hemisphere, R – right hemisphere, Pir – piriform cortex, Amy – amygdala, Prh – perirhinal cortex, DHip – dorsal hippocampus, VHip – ventral hippocampus, Ent – entorhinal cortex.

[5,31,32], the amygdala, contralateral hippocampus, cingulate gyrus, and thalamic nuclei [8,33]. Animal models and human case studies show that in TLE, the seizure can initiate in any limbic structure, even in the same animal or patient, and often, seizures can have a diffuse multi-regional onset [8,9,34,35]. Such a complex network organization explains why the current surgical treatment of TLE, targeting primarily the hippocampus, results in seizure freedom for some patients and why seizures persist even after hippocampus

resection in a substantial patient population. Significantly improving the outcome of epilepsy surgery relies on a better understanding of limbic network organization in appropriate models of these TLE subsyndromes [5].

In this study, we took advantage of a unique feature of the TeNT model of non-lesional temporal lobe epilepsy to explore how spatially limited lesion (unilateral dorsal hippocampal TeNT injection) affects limbic network ictogenesis. The TeNT model is a reliable model of acquired non-lesional TLE, although genetic

models of TLE epilepsy with mild or absent hippocampal damage were also reported [36]. Results showed that single-site TeNT injection leads to widespread limbic network dysfunction. In our study, the network dysfunction manifested by multisite seizure onset that varied across animals. Although the seizures could initiate in any explored limbic structure, the ipsilateral ventral hippocampus played the central role and represented the primary seizure onset zone [37,38]. Past studies that sampled only dorsal hippocampal subregions have already demonstrated widely distributed abnormal network activity in the TeNT model that was manifested mainly by bilateral interictal activity [35]. Interictal epileptiform discharges were generated in both hippocampi in all animals, and interictal discharge rates were higher in the contralateral hippocampus in 40 % of animals. Up to 27 % of seizures originated from the contralateral dorsal hippocampus [35].

The involvement of multiple structures in our model was probably attributed to the functional changes rather than structural changes and cell damage observed in status epilepticus models of TLE [14,39]. Tetanus toxin cleaves two proteins, VAMP-1 and VAMP-2, critical for synaptic transmission [40]. The area of VAMP cleavage is spatially limited to the ipsilateral dorsal hippocampus, leading to the complete absence of spontaneous and evoked inhibitory postsynaptic currents and a significant reduction in excitatory postsynaptic currents [41,42]. The altered synaptic transmission can cause local hippocampal disinhibition and induce disinhibition in distant interconnected structures of limbic circuitry. A decreased excitatory drive from the injected dorsal hippocampus can be associated with reduced feedforward inhibition in a targeted area (entorhinal cortex, contralateral hippocampus). Alternatively, dorsal hippocampal toxin injection may affect long-range inhibition provided by hippocampal interneurons projecting to remote limbic structures [43,44]. This mechanism would explain the presence of entorhinal disinhibition in the chronic epileptic entorhinal cortex that maintains the local inhibition intact [45]. In this scenario, disinhibited distant structures may become active, if not dominant, components of the epileptic network that will substantially contribute to seizure genesis [46,47]. The ventral hippocampus represents a limbic structure (see below) that may be highly susceptible to disinhibition and become the primary seizure-generating structure.

The observed dissociation between the primary

molecular lesion (TeNT injection site) and the major seizure onset zone was unexpected. Our results support the central role of the ventral hippocampus in the pathogenesis of seizures of temporal lobe (limbic) origin. Functional and structural differences between dorsal and ventral hippocampus are well determined, as well as higher epileptogenicity of the ventral hippocampus [48]. Similarly to humans, the rodent hippocampus is divided into functionally distinct regions along its longitudinal axis [49,50]. The rodent ventral hippocampus is homologous to the human anterior hippocampus, the most common seizure initiation site in temporal lobe epilepsy patients [51-56]. Animal models of TLE corroborate this observed intrinsic difference in ictogenicity of ventral and dorsal hippocampal poles, but the underlying cause remains to be fully elucidated.

Ventral and dorsal hippocampus differ in their synaptic input and output and were shown to activate different networks when seizing [57]. The dorsal hippocampus receives polymodal sensory information from the cortex, whereas the ventral hippocampus is more linked to subcortical structures, such as the amygdala and hypothalamus [21]. The trisynaptic circuit of the hippocampus remains conserved along its longitudinal axis, but the circuitry exhibits quantitative differences [24,58,59]. Injection of TeNT or kainic acid into the ventral hippocampus generates a seizure phenotype that is analogous to TLE in humans [12,41,49,60]. In another widely used model of epilepsy using systemic pilocarpine injections, the subsequent seizures were also generated in the ventral hippocampus [9,61]. At a cellular level, CA1 pyramidal neurons in the ventral hippocampus are more depolarized and fire action potentials in response to significantly smaller current injections than dorsal hippocampal neurons [22]. Increased neuronal excitability could result from expression profile differences between the dorsal and ventral hippocampus. In particular, increased ventral hippocampal pyramidal neuron excitability likely relates to the differences in NMDA receptors [24], A-type and KCNQ potassium channels [22,33], different subunit composition of voltage-gated sodium channels [62], and differences in adenosine signaling [63]. An imbalance of excitatory and inhibitory neuron populations might also explain the overall changes in excitability. The loss of GABAergic ventral hippocampal interneurons correlates with the seizure frequency in a mouse model of epilepsy [64]. Similarly, in humans, TLE is associated with more significant cell loss and hippocampal sclerosis in the

homologous anterior hippocampal region [13,65]. Experimentally, local pharmacological suppression of the ventral hippocampal neurons [61] or transplantation of inhibitory neurons [66] successfully reduced the seizure frequency in the systemic pilocarpine model. The ventral hippocampus also plays a pivotal role in TLE with dual pathologies cases where hippocampal sclerosis is associated with focal cortical dysplasia. It is hypothesized that the highly epileptogenic focal cortical dysplasia recruits the susceptible ventral hippocampus, becoming the primary seizure onset zone [6].

Conclusions

This study reveals the complex nature of TLE networks, highlighting the dissociation between the primary lesion and seizure onset zone that, in our observations, manifested as an unexpectedly central role of the ventral hippocampi in seizure initiation. These

findings emphasize the importance of understanding the functional differences between the dorsal and ventral hippocampus and the need for a deeper understanding of the limbic network's organization in different TLE subsyndromes.

Conflict of Interest

There is no conflict of interest.

Acknowledgements

This study was supported by grants of the Czech Science Foundation (20-25298S, 21-17564S), the Ministry of Health of the Czech Republic (NU21-08-00533, NU21-04-00601, NV18-04-00085), the Ministry of Education, Youth and Sports of the Czech Republic (EU – Next Generation EU: LX22NPO5107), and Charles University (PRIMUS 247132). The authors are grateful to CESNET for access to their data storage facility.

References

- Bertram EH. Temporal lobe epilepsy: where do the seizures really begin? *Epilepsy Behav* 2009;14(Suppl 1):32-37. <https://doi.org/10.1016/j.yebeh.2008.09.017>
- Jefferys JGR, Jiruska P, de Curtis M, Avoli M. Limbic Network Synchronization and Temporal Lobe Epilepsy. In: *Jasper's Basic Mechanisms of the Epilepsies*. Noebels JL, Avoli M, Rogawski MA, Olsen RW, Delgado-Escueta AV (Eds.), National Center for Biotechnology Information (US), 2012, Bethesda (MD). <https://doi.org/10.1093/med/9780199746545.003.0014>
- Sutula T, Cascino G, Cavazos J, Parada I, Ramirez L. Mossy fiber synaptic reorganization in the epileptic human temporal lobe. *Ann Neurol* 1989;26:321-330. <https://doi.org/10.1002/ana.410260303>
- Bonilha L, Martz GU, Glazier SS, Edwards JC. Subtypes of medial temporal lobe epilepsy: influence on temporal lobectomy outcomes? *Epilepsia* 2012;53:1-6. <https://doi.org/10.1111/j.1528-1167.2011.03298.x>
- Thom M, Mathern GW, Cross JH, Bertram EH. Mesial temporal lobe epilepsy: How do we improve surgical outcome? *Ann Neurol* 2010;68:424-434. <https://doi.org/10.1002/ana.22142>
- Blümcke I, Coras R, Miyata H, Ozkara C. Defining clinico-neuropathological subtypes of mesial temporal lobe epilepsy with hippocampal sclerosis. *Brain Pathol* 2012;22:402-411. <https://doi.org/10.1111/j.1750-3639.2012.00583.x>
- Bertram EH. Why does surgery fail to cure limbic epilepsy? *Epilepsy Res* 2003;56:93-99. <https://doi.org/10.1016/j.eplepsyres.2003.10.003>
- Bertram EH, Zhang DX, Mangan P, Fountain N, Rempe D. Functional anatomy of limbic epilepsy: a proposal for central synchronization of a diffusely hyperexcitable network. *Epilepsy Res* 1998;32:194-205. [https://doi.org/10.1016/S0920-1211\(98\)00051-5](https://doi.org/10.1016/S0920-1211(98)00051-5)
- Toyoda I, Bower MR, Leyva F, Buckmaster PS. Early activation of ventral hippocampus and subiculum during spontaneous seizures in a rat model of temporal lobe epilepsy. *Pol J Pharmacol Pharm* 2013;33:11100-11115. <https://doi.org/10.1523/JNEUROSCI.0472-13.2013>
- Télez-Zenteno JF, Hernández Ronquillo L, Moien-Afshari F, Wiebe S. Surgical outcomes in lesional and non-lesional epilepsy: a systematic review and meta-analysis. *Epilepsy Res* 2010;89:310-318. <https://doi.org/10.1016/j.eplepsyres.2010.02.007>

11. Barba C, Barbati G, Minotti L, Hoffmann D, Kahane P. Ictal clinical and scalp-EEG findings differentiating temporal lobe epilepsies from temporal 'plus' epilepsies. *Brain* 2007;130(Pt 7):1957-1967. <https://doi.org/10.1093/brain/awm108>
12. Cavalheiro EA, Riche DA, Le Gal La Salle G. Long-term effects of intrahippocampal kainic acid injection in rats: a method for inducing spontaneous recurrent seizures. *Electroencephalogr Clin Neurophysiol* 1982;53:581-589. [https://doi.org/10.1016/0013-4694\(82\)90134-1](https://doi.org/10.1016/0013-4694(82)90134-1)
13. Ekstrand JJ, Pouliot W, Scheerlinck P, Dudek FE. Lithium pilocarpine-induced status epilepticus in postnatal day 20 rats results in greater neuronal injury in ventral versus dorsal hippocampus. *Neuroscience* 2011;192:699-707. <https://doi.org/10.1016/j.neuroscience.2011.05.022>
14. Pitkanen A, Schwartzkroin PA, Moshe SL. *Models of Seizures and Epilepsy 1st edition*. Academic Press Inc (London), London, England, 2006.
15. Turski L, Cavalheiro EA, Czuczwar SJ, Turski WA, Kleinrok Z. The seizures induced by pilocarpine: behavioral, electroencephalographic and neuropathological studies in rodents. *Pol J Pharmacol Pharm* 1987;39:545-555.
16. Turski WA, Cavalheiro EA, Schwarz M, Czuczwar SJ, Kleinrok Z, Turski L. Limbic seizures produced by pilocarpine in rats: behavioral, electroencephalographic and neuropathological study. *Behav Brain Res* 1983;9:315-335. [https://doi.org/10.1016/0166-4328\(83\)90136-5](https://doi.org/10.1016/0166-4328(83)90136-5)
17. Williams PA, White AM, Clark S, Ferraro DJ, Swiercz W, Staley KJ, Dudek FE. Development of spontaneous recurrent seizures after kainate-induced status epilepticus. *J Neurosci* 2009;29:2103-2112. <https://doi.org/10.1523/JNEUROSCI.0980-08.2009>
18. Sloviter RS. The neurobiology of temporal lobe epilepsy: too much information, not enough knowledge. *C R Biol* 2005;328:143-153. <https://doi.org/10.1016/j.crv.2004.10.010>
19. Jefferys JG, Evans BJ, Hughes SA, Williams SF. Neuropathology of the chronic epileptic syndrome induced by intrahippocampal tetanus toxin in rat: preservation of pyramidal cells and incidence of dark cells. *Neuropathol Appl Neurobiol* 1992;18:53-70. <https://doi.org/10.1111/j.1365-2990.1992.tb00764.x>
20. Jiruska P, Shtaya ABY, Bodansky DMS, Chang WC, Gray WP, Jefferys JGR. Dentate gyrus progenitor cell proliferation after the onset of spontaneous seizures in the tetanus toxin model of temporal lobe epilepsy. *Neurobiol Dis* 2013;54:492-498. <https://doi.org/10.1016/j.nbd.2013.02.001>
21. Bannerman DM, Sprengel R, Sanderson DJ, McHugh SB, Rawlins JNP, Monyer H, Seeburg PH. Hippocampal synaptic plasticity, spatial memory and anxiety. *Nat Rev Neurosci* 2014;15:181-192. <https://doi.org/10.1038/nrn3677>
22. Dougherty KA, Islam T, Johnston D. Intrinsic excitability of CA1 pyramidal neurones from the rat dorsal and ventral hippocampus. *J Physiol* 2012;590:5707-5722. <https://doi.org/10.1113/jphysiol.2012.242693>
23. Dougherty KA, Nicholson DA, Diaz L, Buss EW, Neuman KM, Chetkovich DM, Johnston D. Differential expression of HCN subunits alters voltage-dependent gating of h-channels in CA1 pyramidal neurons from dorsal and ventral hippocampus. *J Neurophysiol* 2013;109:1940-1953. <https://doi.org/10.1152/jn.00010.2013>
24. Papatheodoropoulos C, Moschovos C, Kostopoulos G. Greater contribution of N-methyl-D-aspartic acid receptors in ventral compared to dorsal hippocampal slices in the expression and long-term maintenance of epileptiform activity. *Neuroscience* 2005;135:765-779. <https://doi.org/10.1016/j.neuroscience.2005.06.024>
25. Paxinos G, Watson C. *The Rat Brain in Stereotaxic Coordinates 6th Edition*. Elsevier, 2007.
26. Racine RJ. Modification of seizure activity by electrical stimulation. II. Motor seizure. *Electroencephalogr Clin Neurophysiol* 1972;32:281-294. [https://doi.org/10.1016/0013-4694\(72\)90177-0](https://doi.org/10.1016/0013-4694(72)90177-0)
27. Avanzini G, Manganotti P, Meletti S, Moshé SL, Panzica F, Wolf P, Capovilla G. The system epilepsies: a pathophysiological hypothesis. *Epilepsia* 2012;53:771-778. <https://doi.org/10.1111/j.1528-1167.2012.03462.x>
28. Holmes MD, Dodrill CB, Ojemann GA, Wilensky AJ, Ojemann LM. Outcome following surgery in patients with bitemporal interictal epileptiform patterns. *Neurology* 1997;48:1037-1040. <https://doi.org/10.1212/WNL.48.4.1037>
29. Jiruska P, de Curtis M, Jefferys JGR. Modern concepts of focal epileptic networks. *Int Rev Neurobiol* 2014;114:1-7. <https://doi.org/10.1016/B978-0-12-418693-4.00001-7>
30. Reid AY, Staba RJ. Limbic networks: clinical perspective. *Int Rev Neurobiol* 2014;114:89-120. <https://doi.org/10.1016/B978-0-12-418693-4.00005-4>
31. Avoli M, D'Antuono M, Louvel J, Köhling R, Biagini G, Pumain R, D'Arcangelo G, Tancredi V. Network and pharmacological mechanisms leading to epileptiform synchronization in the limbic system in vitro. *Prog Neurobiol* 2002;68:167-207. [https://doi.org/10.1016/S0301-0082\(02\)00077-1](https://doi.org/10.1016/S0301-0082(02)00077-1)

32. Barbarosie M, Avoli M. CA3-driven hippocampal-entorhinal loop controls rather than sustains in vitro limbic seizures. *J Neurosci* 1997;17:9308-9314. <https://doi.org/10.1523/JNEUROSCI.17-23-09308.1997>
33. Levesque M, Salami P, Behr C, Avoli M. Temporal lobe epileptiform activity following systemic administration of 4-aminopyridine in rats. *Epilepsia* 2013;54:596-604. <https://doi.org/10.1111/epi.12041>
34. Finnerty GT, Jefferys JGR. Investigation of the neuronal aggregate generating seizures in the rat tetanus toxin model of epilepsy. *J Neurophysiol* 2002;88:2919-2927. <https://doi.org/10.1152/jn.00211.2002>
35. Jiruska P, Finnerty GT, Powell AD, Lofti N, Cmejla R, Jefferys JGR. Epileptic high-frequency network activity in a model of non-lesional temporal lobe epilepsy. *Brain* 2010;133:1380-1390. <https://doi.org/10.1093/brain/awq070>
36. King JT Jr, LaMotte CC. El mouse as a model of focal epilepsy: a review. *Epilepsia* 1989;30:257-265. <https://doi.org/10.1111/j.1528-1157.1989.tb05296.x>
37. Kahane P, Landré E, Minotti L, Francione S, Ryvlin P. The Bancaud and Talairach view on the epileptogenic zone: a working hypothesis. *Epileptic Disord* 2006;8(Suppl 2):S16-S26.
38. Rosenow F, Lüders H. Presurgical evaluation of epilepsy. *Brain* 2001;124:1683-1700. <https://doi.org/10.1093/brain/124.9.1683>
39. Pitkänen A, Engel J Jr. Past and present definitions of epileptogenesis and its biomarkers. *Neurotherapeutics* 2014;11:231-241. <https://doi.org/10.1007/s13311-014-0257-2>
40. Schiavo G, Rossetto O, Benfenati F, Poulain B, Montecucco C. Tetanus and botulinum neurotoxins are zinc proteases specific for components of the neuroexocytosis apparatus. *Ann N Y Acad Sci* 1994;710:65-75. <https://doi.org/10.1111/j.1749-6632.1994.tb26614.x>
41. Ferecskó AS, Jiruska P, Foss L, Powell AD, Chang W-C, Sik A, Jefferys JGR. Structural and functional substrates of tetanus toxin in an animal model of temporal lobe epilepsy. *Brain Struct Funct* 2015;220:1013-1029. <https://doi.org/10.1007/s00429-013-0697-1>
42. Jefferys JG. Chronic epileptic foci in vitro in hippocampal slices from rats with the tetanus toxin epileptic syndrome. *J Neurophysiol* 1989;62:458-468. <https://doi.org/10.1152/jn.1989.62.2.458>
43. Chrobak JJ, Buzsáki G. High-frequency oscillations in the output networks of the hippocampal-entorhinal axis of the freely behaving rat. *J Neurosci* 1996;16:3056-3066. <https://doi.org/10.1523/JNEUROSCI.16-09-03056.1996>
44. Urrutia-Piñones J, Morales-Moraga C, Sanguinetti-González N, Escobar AP, Chiu CQ. Long-Range GABAergic Projections of Cortical Origin in Brain Function. *Front Syst Neurosci* 2022;16:841869. <https://doi.org/10.3389/fnsys.2022.841869>
45. Fountain NB, Bear J, Bertram EH 3rd, Lothman EW. Responses of deep entorhinal cortex are epileptiform in an electrogenic rat model of chronic temporal lobe epilepsy. *J Neurophysiol* 1998;80:230-240. <https://doi.org/10.1152/jn.1998.80.1.230>
46. Empson RM, Jefferys JG. Synaptic inhibition in primary and secondary chronic epileptic foci induced by intrahippocampal tetanus toxin in the rat. *J Physiol* 1993;465:595-614. <https://doi.org/10.1113/jphysiol.1993.sp019695>
47. Najlerahim A, Williams SF, Pearson RC, Jefferys JG. Increased expression of GAD mRNA during the chronic epileptic syndrome due to intrahippocampal tetanus toxin. *Exp Brain Res* 1992;90:332-342. <https://doi.org/10.1007/BF00227246>
48. Fanselow MS, Dong H-W. Are the dorsal and ventral hippocampus functionally distinct structures? *Neuron* 2010;65:7-19. <https://doi.org/10.1016/j.neuron.2009.11.031>
49. Mellanby J, George G, Robinson A, Thompson P. Epileptiform syndrome in rats produced by injecting tetanus toxin into the hippocampus. *J Neurol Neurosurg Psychiatry* 1977;40:404-414. <https://doi.org/10.1136/jnmp.40.4.404>
50. Moser MB, Moser EI. Functional differentiation in the hippocampus. *Hippocampus* 1998;8:608-619. [https://doi.org/10.1002/\(SICI\)1098-1063\(1998\)8:6<608::AID-HIPO3>3.0.CO;2-7](https://doi.org/10.1002/(SICI)1098-1063(1998)8:6<608::AID-HIPO3>3.0.CO;2-7)
51. Masukawa LM, O'Connor WM, Lynott J, Burdette LJ, Uruno K, McGonigle P, O'Connor MJ. Longitudinal variation in cell density and mossy fiber reorganization in the dentate gyrus from temporal lobe epileptic patients. *Brain Res* 1995;678:65-75. [https://doi.org/10.1016/0006-8993\(95\)00167-O](https://doi.org/10.1016/0006-8993(95)00167-O)
52. Quesney LF. Clinical and EEG features of complex partial seizures of temporal lobe origin. *Epilepsia* 1986;27(Suppl 2):S27-S45. <https://doi.org/10.1111/j.1528-1157.1986.tb05738.x>
53. So N, Gloor P, Quesney LF, Jones-Gotman M, Olivier A, Andermann F. Depth electrode investigations in patients with bitemporal epileptiform abnormalities. *Ann Neurol* 1989;25:423-431. <https://doi.org/10.1002/ana.410250502>

54. Spencer SS. Neural networks in human epilepsy: evidence of and implications for treatment. *Epilepsia* 2002;43:219-227. <https://doi.org/10.1046/j.1528-1157.2002.26901.x>
55. Spencer SS, Spencer DD. Entorhinal-hippocampal interactions in medial temporal lobe epilepsy. *Epilepsia* 1994;35:721-727. <https://doi.org/10.1111/j.1528-1157.1994.tb02502.x>
56. Wennberg R, Arruda F, Quesney LF, Olivier A. Preeminence of extrahippocampal structures in the generation of mesial temporal seizures: evidence from human depth electrode recordings. *Epilepsia* 2002;43:716-726. <https://doi.org/10.1046/j.1528-1157.2002.31101.x>
57. Duffy BA, Choy M, Lee JH. Predicting Successful Generation and Inhibition of Seizure-like Afterdischarges and Mapping Their Seizure Networks Using fMRI. *Cell Rep* 2020;30:2540-2554.e4. <https://doi.org/10.1016/j.celrep.2020.01.095>
58. Pandis C, Sotiriou E, Kouvaras E, Asproдини E, Papatheodoropoulos C, Angelatou F. Differential expression of NMDA and AMPA receptor subunits in rat dorsal and ventral hippocampus. *Neuroscience* 2006;140:163-175. <https://doi.org/10.1016/j.neuroscience.2006.02.003>
59. Sotiriou E, Papatheodoropoulos C, Angelatou F. Differential expression of gamma-aminobutyric acid--a receptor subunits in rat dorsal and ventral hippocampus. *J Neurosci Res* 2005;82:690-700. <https://doi.org/10.1002/jnr.20670>
60. Jefferys JGR, Ashby-Lumsden A, Lovick TA. Cardiac effects of repeated focal seizures in rats induced by intrahippocampal tetanus toxin: Bradyarrhythmias, tachycardias, and prolonged interictal QT interval. *Epilepsia* 2020;61:798-809. <https://doi.org/10.1111/epi.16479>
61. Buckmaster PS, Reyes B, Kahn T, Wyeth M. Ventral hippocampal formation is the primary epileptogenic zone in a rat model of temporal lobe epilepsy. *J Neurosci* 2022;42:7482-7495. <https://doi.org/10.1523/JNEUROSCI.0429-22.2022>
62. Cembrowski MS, Wang L, Sugino K, Shields BC, Spruston N. HippoSeq: a comprehensive RNA-seq database of gene expression in hippocampal principal neurons. *Elife* 2016;5:e14997. <https://doi.org/10.7554/eLife.14997>
63. Moschovos C, Kostopoulos G, Papatheodoropoulos C. Endogenous adenosine induces NMDA receptor-independent persistent epileptiform discharges in dorsal and ventral hippocampus via activation of A2 receptors. *Epilepsy Res* 2012;100:157-167. <https://doi.org/10.1016/j.epilepsyres.2012.02.012>
64. Wyeth M, Nagendran M, Buckmaster PS. Ictal onset sites and γ -aminobutyric acidergic neuron loss in epileptic pilocarpine-treated rats. *Epilepsia* 2020;61:856-867. <https://doi.org/10.1111/epi.16490>
65. Babb TL, Brown WJ, Pretorius J, Davenport C, Lieb JP, Crandall PH. Temporal lobe volumetric cell densities in temporal lobe epilepsy. *Epilepsia* 1984;25:729-740. <https://doi.org/10.1111/j.1528-1157.1984.tb03484.x>
66. Hunt RF, Girsakis KM, Rubenstein JL, Alvarez-Buylla A, Baraban SC. GABA progenitors grafted into the adult epileptic brain control seizures and abnormal behavior. *Nat Neurosci* 2013;16:692-697. <https://doi.org/10.1038/nn.3392>